Transonic Aeroelastic Analysis of the B-1 Wing

Guru P. Guruswamy*
Sterling Software/Informatics, Palo Alto, California
Peter M. Goorjian†
NASA Ames Research Center, Moffett Field, California
and
Hiroshi Ide‡ and Gerry D. Miller‡
Rockwell International, Los Angeles, California

The flow over the B-1 wing is studied computationally, including the aeroelastic response of the wing. Computed results are compared with results from wind tunnel and flight tests for both low- and high-sweep cases, at 25.0 and 67.5 deg, respectively, for selected transonic Mach numbers. The aerodynamic and aeroelastic computations are made by using the transonic unsteady code ATRAN3S. Steady aerodynamic computations compare well with wind tunnel results for the 25.0 deg sweep case and also for small angles of attack at 67.5 deg sweep case. The aeroelastic response results show that the wing is stable at the low-sweep angle for the calculation at the Mach number at which there is a shock wave. In the higher-sweep case, for the higher angle of attack at which oscillations were observed in the flight and wind tunnel tests, the calculations do not show any shock waves. Their absence lends support to the hypothesis that the observed oscillations are due to the presence of leading-edge separation vortices and not to shock wave motion, as was previously proposed.

Introduction

THE variable sweep B-1 wing has been observed to undergo aeroelastic oscillations dependent on the angle of attack in both flight and wind tunnel tests.[1,2] These oscillations occurred in the transonic regime, but outside the present actual flight envelope of the B-1 aircraft at both low- and high-sweep angles. Motivated by these observations, in this paper the flow over the B-1 wing is studied computationally, including the aeroelastic response of the wing. Computed results are compared with results from the wind tunnel and flight tests for both the low- and high-sweep cases. In the low-sweep case, the comparisons demonstrate the capability of the computational methods to properly simulate the flow in the presence of shock waves. In the high-sweep case, where the sweep angle is equal to 67.5 deg, the comparisons at a low angle of attack demonstrate the capability of the computational methods to properly simulate the flow at an extreme sweep angle. Finally, a comparison is presented in the high-sweep case of a higher angle of attack at which oscillations were observed. The calculations do not show any shock waves, an absence that lends support to the interpretation of the data measured in a parallel wind tunnel test.[2]

To study the transonic aeroelastic characteristics of wings, efficient computational tools are required to compute unsteady flows over wings. There is an extensive effort in the area of computational fluid dynamics (CFD)[3] to develop methods for transonic unsteady aerodynamics. To date, methods based on the small-disturbance potential theory[4] are being routinely used in two-dimensional aeroelastic analysis.[5] The use of three-dimensional methods for practical wings has begun.

Presented as Paper 85-0690 at the AIAA/ASME/ASCE/AHS 26th Structures, Structural Dynamics and Materials Conference, Orlando, FL, April 15-17, 1985; received April 27, 1985; revision received March 25, 1986. This paper is declared a work of the U.S. Government and is not subject to copyright protection in the United States.

*Principal Analyst. Member AIAA.
†Research Scientist. Associate Fellow AIAA.
‡Member, Technical Staff. Member AIAA.

An unsteady, small-disturbance transonic code called XTRAN3S based on a time-integration method was developed by Borland and Rizzetta[6] as an extension to three dimensions. Also, this code has the capability of conducting static and dynamic aeroelastic computations by simultaneously integrating the aerodynamic and structural equations of motion. The authors illustrated the capability of XTRAN3S by computing flutter boundaries for a rectangular wing with a 6% thick parabolic-arc airfoil section at transonic Mach numbers. Guruswamy and Goorjian[7] and Seidel et al.[8] have illustrated the applications to other rectangular wings, and Myers et al.[9] have illustrated the applications to a transport wing with an aspect ratio of 8, a taper ratio of 0.4, and a leading-edge sweep angle of 20 deg.

The use of the original version of XTRAN3S was limited to wings with high-aspect ratios, large-taper ratios, and small sweep angles because of the nature of coordinate transformation employed. Guruswamy and Goorjian[10] developed an alternate efficient coordinate transformation that is incorporated in ATRAN3S. ATRAN3S is a modified version of XTRAN3S with many other new features. As a result, ATRAN3S makes computations faster, more accurate, and more stable than XTRAN3S as illustrated in Ref. 10 for the F-5 wing, which is a low aspect ratio, small taper ratio, high-sweep fighter wing. An improved version of viscous corrections that were originally implemented in XTRAN3S by Rizzetta and Borland[11] are present in ATRAN3S. The viscous computing capability of ATRAN3S was illustrated by Guruswamy et al.[12] for a rectangular wing and a typical transport wing.

In this work, a transonic aeroelastic analysis is conducted for the B-1 wing, which is a variable-sweep wing. The sweep angle of the wing is 15-67.5 deg and the aircraft cruises in the transonic regime. Flight tests on the wing and wind tunnel tests[2] on the 1/10 scale model of the wing showed zero damped aeroelastic oscillations dependent on the angle of attack. In a recent aeroelastic model experiment conducted in the NASA Ames 11 × 11 ft Transonic Wind Tunnel,[2] significant aeroelastic limited oscillations in the wing-first bending mode were observed in the higher transonic regime over a narrow band of angles of attack. Those oscillations occurred

at high-sweep angles of around 65 deg. At the sweep angle of 25 deg, some small aeroelastic oscillations were also observed, which were attributed to aerodynamic buffeting.

Motivated by these observations, the flow over the B-1 wing is studied computationally, including the aeroelastic response of the wing. For this purpose, the NASA Ames Research Center, transonic, unsteady, code ATRAN3S is used. Aerodynamic and aeroelastic analyses are conducted at two sweep angles, 25.0 and 67.5 deg, for selected Mach numbers and the results are compared with wind tunnel and flight results.

Transonic Aerodynamic Equations of Motion

In this analysis the modified unsteady three-dimensional transonic small-disturbance equation is employed,

$$A\phi_{tt} + B\phi_{xt} = [E\phi_x + F\phi_x^2 + G\phi_y^2]_x + [\phi_y + H\phi_x\phi_y]_y + [\phi_z]_z \quad (1)$$

where

$$A = M_\infty^2, \qquad B = 2M_\infty^2 \qquad E = 1 - M_\infty^2,$$

$$F = -\tfrac{1}{2}(\gamma+1)M_\infty^2, \qquad G = -\tfrac{1}{2}(\gamma-3)M_\infty^2,$$

$$H = -(\gamma-1)M_\infty^2$$

This equation is solved in the computer code ATRAN3S by a time-accurate finite difference scheme that employs an alternating direction implicit (ADI) algorithm.[4] Whereas ATRAN3S employs the modified coordinate transformation technique,[10] it is noted here that the conventional transformation originally employed in XTRAN3S[6] is not adequate for the high-sweep case of the B-1 wing. During the course of this work, ATRAN3S was further improved by modifying the code to implicitly treat some additional terms in the finite difference form of Eq. (1) in order to improve the stability of the algorithm. This speeded up the code by a factor of two for subsonic cases.

For all cases considered in this study, a grid with 64 points in the streamwise direction, 40 points in the vertical direction, and 20 points in the spanwise direction was employed. The wing surface was defined by 39 points in the streamwise direction and 13 points in the spanwise direction. Computational boundaries were located as follows: the upstream boundary was at 15 chords, the downstream boundary at 25 chords, the far span boundary at 1.6 semispans, above the wing the grid boundary at 25 chords, and below the wing the grid boundary at 25 chords.

Aeroelastic Equations of Motion

The governing aeroelastic equations of motion of a flexible wing are obtained by using the Rayleigh-Ritz method (see Ref. 13, Chap. 3). In this method, the resulting aeroelastic displacements at any time are expressed as a function of a finite set of assumed modes. The contribution of each assumed mode to the total motion is derived by Lagrange's equation. Further, it is assumed that the deformation of the continuous wing structure can be represented by deflections at a set of discrete points. This assumption facilitates the use of discrete structural data, such as the modal vector, the modal stiffness matrix, and the modal mass matrix. These are generated by a finite element analysis or by experimental influence coefficient measurements.

The final matrix form of the aeroelastic equations of motion is

$$[M]\{\ddot{q}\} + [G]\{\dot{q}\} + [K]\{q\} = \{F\} \quad (2)$$

where

$$\{F\} = 1/2\rho U_\infty^2 [\phi_A]^T [A]\{\Delta C_p\}$$

is the aerodynamic force vector, $[\phi_A]$ the modal matrix, and $[A]$ the diagonal area matrix of the aerodynamic control points.

These equations of motion are solved by numerically integrating Eq. (2) in time by the linear acceleration method, which is the same as the explicit finite difference Euler method. Detailed illustration of the method for the aeroelastic analysis airfoils is given in Ref. 5. The method is briefly described here.

The step-by-step integration procedure for obtaining the aeroelastic response was carried out as follows. Assuming freestream conditions and wing surface boundary conditions obtained from a set of selected starting values of the generalized displacement, velocity, and acceleration vectors, the generalized aerodynamic force vector $F(t)$ at time $t+\Delta t$ was computed by solving Eq. (1). Using this aerodynamic vector, the generalized displacement, velocity, and acceleration vectors for the time level $t+\Delta t$ are calculated by numerically integrating Eq. (2). From the generalized coordinates computed at the time level $t+\Delta t$, the new boundary conditions on the surface of the wing are computed. With these new boundary conditions the aerodynamic vector $F(t)$ at the next time level is computed by using Eq. (1). This process is repeated every time step to solve the aerodynamic and structural equations of motion forward in time until the required response is obtained.

Results: Modeling the Wing for the Analysis

A schematic diagram of the B-1 aircraft is given in Fig. 1. From this configuration, isolated wing planforms are modeled without the glove to represent the aerodynamic and structural characteristics of the wing as closely as possible. The two planforms modeled for sweep angles of 25.0 and 67.5 deg, along with the approximate locations of the glove, are shown in Fig. 2. The four semispan stations along which the computed pressures were compared with those measured in the experiment are also shown in Fig. 2. For both cases, the wing root is located at the pivot point of the wing. The resulting aspect ratio and taper ratio for the 25.0 deg sweep case are 8.26 and 0.41 and the corresponding values for the 67.5 deg sweep case are 1.85 and 0.38, respectively.

Vibrational Analysis

In this analysis, the assumed modes used in Eq. (2) were taken from the natural modes of the wing as determined from a vibrational analysis. The data for the vibrational analysis was prepared from the measured structural stiffnesses and the mass distributions of the wing. The first six natural modes were selected to represent the wing for the aeroelastic analysis. The modes and their associated frequencies that were determined by the vibrational analysis, along with the frequencies of the actual wing from ground vibration tests of the B-1 aircraft, are given in Fig. 3. The frequencies from the vibration analysis on the model planform

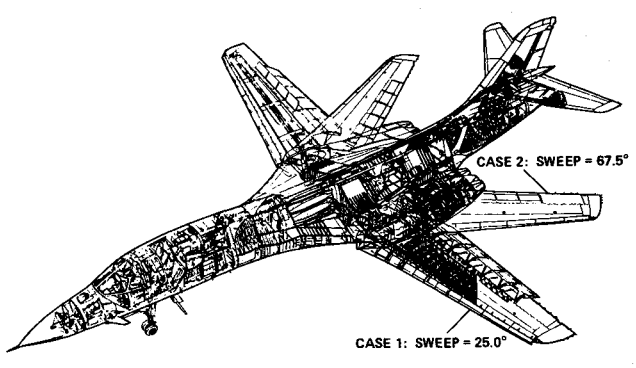

Fig. 1 B-1 aircraft.

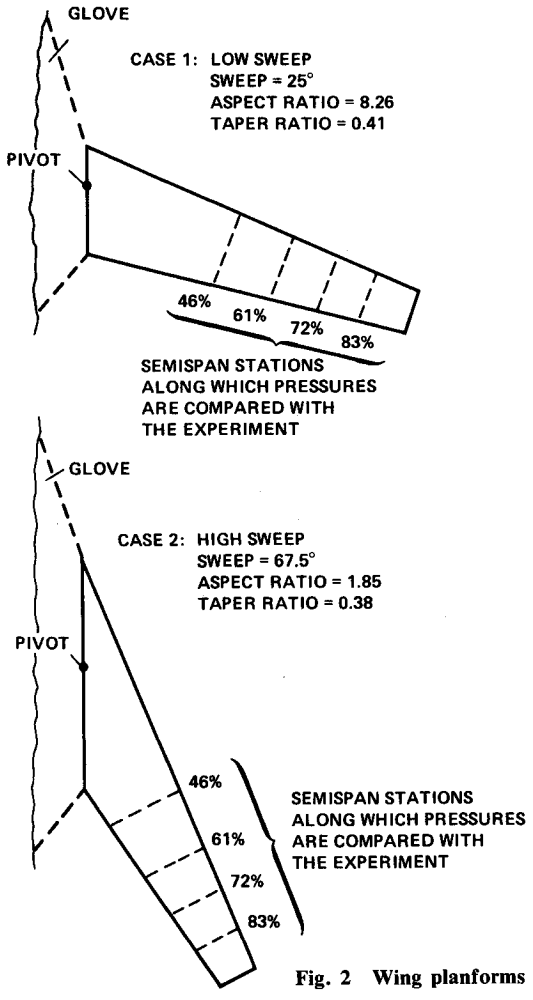

Fig. 2 Wing planforms for analysis.

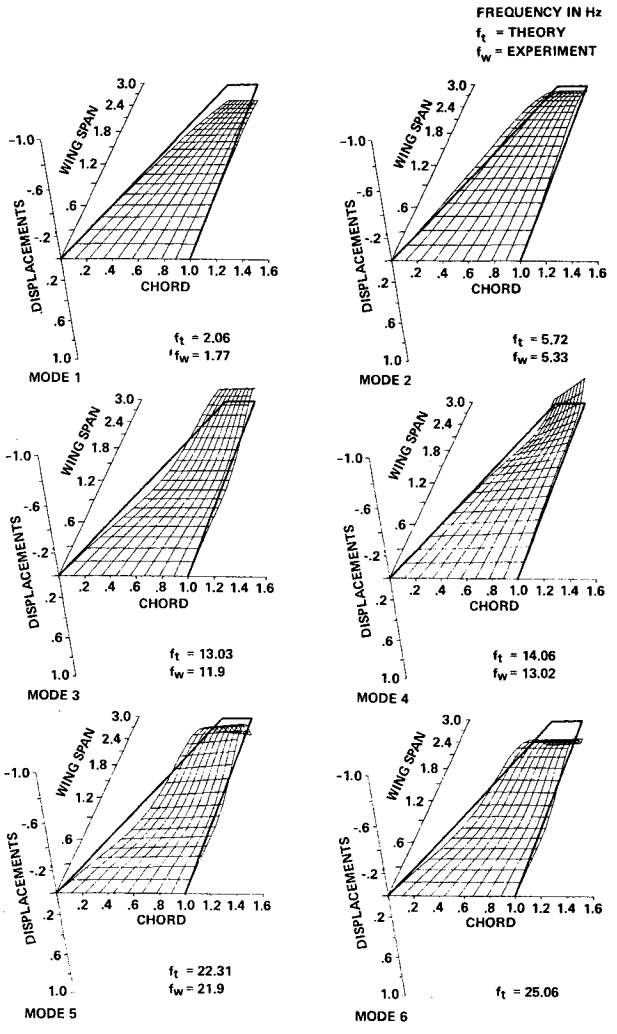

Fig. 3 Six natural vibrational modes.

of the wing prepared for the code are close to those measured for the actual wing in the ground vibration test, as shown in Fig. 3. Thus, the model in the code closely represents the structural characteristics of the actual wing.

Steady Aerodynamic Analysis

Steady aerodynamic computations were made in order to verify that the modeling of the wing was adequate for representation of the actual aerodynamic characteristics of the wing. This verification was made by comparing the results from ATRAN3S with the wind tunnel results measured at the NASA Ames 11×11 ft tunnel on a 1/10 scale model of the wing.[2]

Steady aerodynamic pressures were computed by integrating Eq. (1) in time and setting the steady boundary conditions on the wing. The time step size required for the computation depended mainly upon the sweep angle. The time step sizes required for the 25.0 and 67.5 deg sweep cases were 0.02 and 0.002, respectively.

Steady-state computations were made for subsonic and transonic Mach numbers equal to 0.65 and 0.75, respectively, at the sweep angle of 25 deg. Steady pressure distributions are compared with the experiment at four semispan stations along the sections perpendicular to the elastic axis at 46, 61, 72, and 83% locations. Figure 4 shows the steady pressure distribution at $M=0.65$ and $\alpha=0.0$ deg where the flow is subsonic. As expected, the ATRAN3S results compare well with the experiment. Figure 5 shows the comparison of steady pressure distributions at $M=0.75$ and $\alpha=4.11$ deg. The results compare well between the code and the experiment for all span stations. These close comparisons between the code and the experiment show that the planform

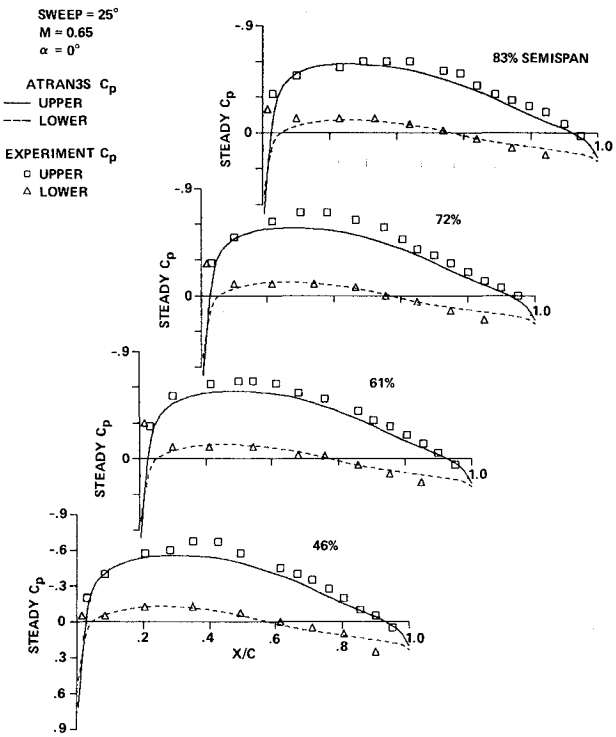

Fig. 4 Steady pressure distributions for the 25 deg sweep case at $M=0.65$.

modeled in Fig. 2 without the glove for the sweep of 25 deg is adequate to aerodynamically represent the wing.

Steady-state computations were then made for several Mach numbers of 0.80-0.873 at various angles of attack for the sweep angle of 67.5 deg. The physical grid required to make computations is shown in Fig. 6. Note the scale in the span direction was stretched by a factor of 10 in Fig. 6a in order to show the details of the grid. In the actual grid, the wing appears swept back by 67.5 deg, as shown in Fig. 6b. It is noted here that the physical grid generated by the original XTRAN3S[6] is not adequate[10] for this high-sweep case. Because of the high sweep and associated low Mach numbers normal to the leading edge, flow in the code remained subsonic for all of the cases considered. The code compared fairly well with the experiment at small angles of attack. For example, Fig. 7 shows steady pressure comparisons between the code and the experiment at four semispan stations along sections perpendicular to the elastic axis at 46, 61, 72, and 83% locations at $M=0.873$ (see Fig. 2) and $\alpha=2.06$ deg. Except for some differences near the leading edge, the comparisons are favorable for all span stations except the 46% semispan one. The disagreement at the 46% semispan is due to the presence of the glove close to that span station (see Fig. 2) in the wind tunnel and the glove is not modeled in the code.

For the high sweep angle of 67.5 deg, at higher angles of attack, both in flight tests and in wind tunnel tests, the wings were observed to undergo oscillations.[1,2] For the flight tests, the oscillations occurred in the range of 8.1-8.4 deg in the angle of attack and for the wind tunnel tests the oscillations occurred at 7.44 deg. It has been proposed in Ref. 1 that the oscillations were due to the motion of shock waves.

To determine whether the shock waves were contributing to the oscillation, calculations were performed at $M=0.80$ and $\alpha=6.0$ and 11.0 deg. At these angles of attack, the wind tunnel data showed none of the oscillations—the calculations should indicate the presence of shock waves if they are there. However, the code ATRAN3S models the flow by a velocity potential as shown in Eq. (1) and hence cannot account for the presence of vortices in the flow. Figure 8 shows the comparison at $\alpha=6.0$ deg between wind tunnel test results and the calculations. The calculations show no sign of the presence of shock waves and differ significantly from the experimental results. Figure 9 shows the computed results at $\alpha=11.0$ deg. It is noted that the small-disturbance theory may be less accurate for this case and should produce a stronger shock wave if the flow is transonic. Again, there is no sign of the presence of shock waves and the results differ significantly from the experimental results reported in Ref. 2. Hence, there are probably no shock waves present at the intermediate angle of attack of 7.44 deg at which the oscillations were observed. To properly model the flow in these cases, where leading-edge vortices are apparently present[2] and the effects of separation are important in understanding the oscillations, a Navier-Stokes code must be used. (See Appendix for more discussion about the formation of vortices.)

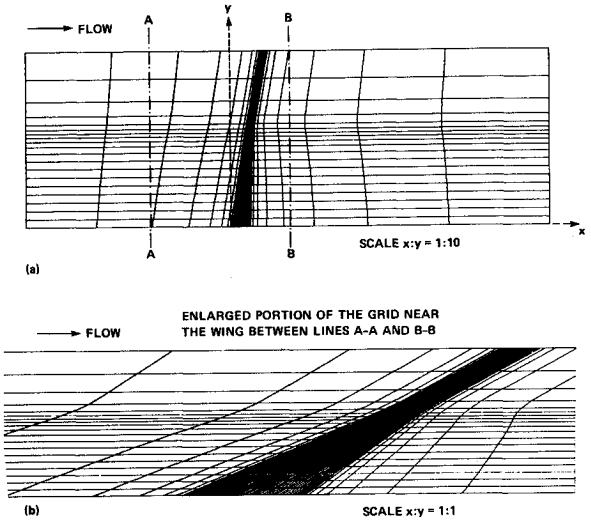

Fig. 6 Physical grid for the 67.5 deg sweep case: a) full grid; b) enlargement near wing.

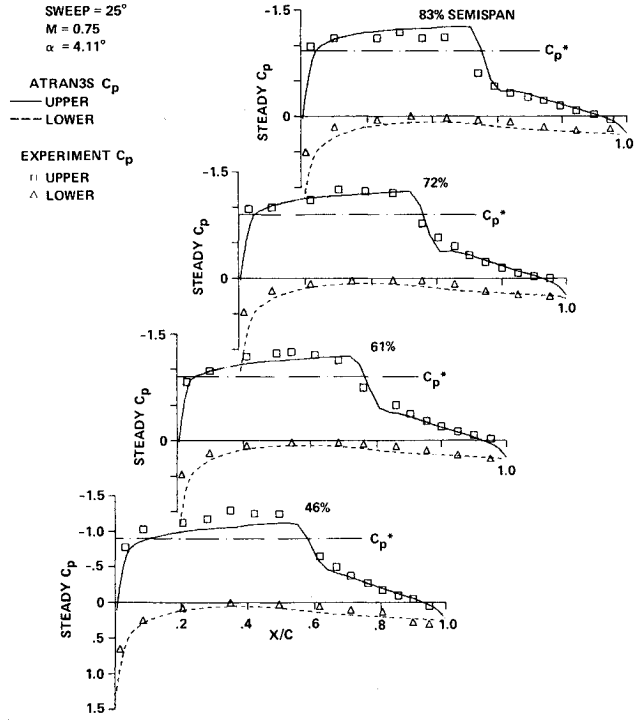

Fig. 5 Steady pressure distributions for the 25 deg sweep case at $M=0.75$.

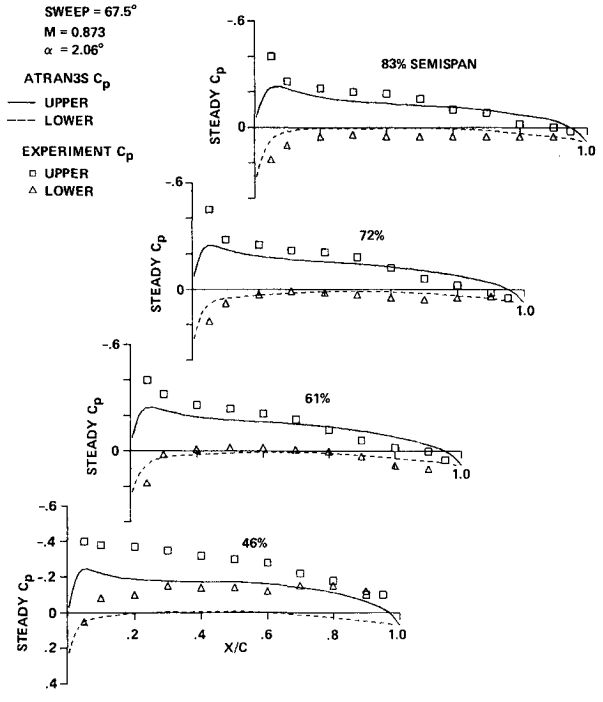

Fig. 7 Steady pressure distributions for the 67.5 deg sweep case at $M=0.873$ and $\alpha=2.06$ deg.

Aeroelastic Response Analysis

In this section, several calculations will be presented that simulate the aeroelastic response of the wing by simultaneously integrating Eqs. (1) and (2). The first case will examine the response of the wing at low sweep under the subsonic flow conditions given in Fig. 4. A transonic case will be computed at the low-sweep angle to determine the presence of shock waves. Finally, a subsonic case will be computed at the high-sweep angle, under the flow conditions given in Fig. 7, to examine the change in the response of the wing as the sweep angle is increased.

For the first case, an aeroelastic analysis is conducted at the subsonic Mach number of 0.65 and $\alpha = 0.0$ deg in order to study the nature of subsonic response of the wing. In this case, the steady pressures from the code compared well with the experiment as shown in Fig. 4. Flow parameters are taken for an altitude of 33,000 ft. The response computations were initiated by giving an arbitrary unit displacement to the first generalized coordinate $q(1)$. The aerodynamic and structural equations of motion were then simultaneously integrated in time until a steady aeroelastic equilibrium state was approached. This required about 10,000 time steps of size 0.02, which corresponds to 6.0 s of physical time at the altitude of 33,000 ft.

In order to simulate an external disturbance to initiate oscillations, an instantaneous change of 2.0 deg to the mean angle of attack was given to the wing and the response computations were further continued. After initial oscillations, the wing again approached a steady aeroelastic equilibrium position. This required about 5000 time steps. Similar responses were repeated for 4.0 deg of instantaneous change in the angle of attack. These responses for the first normal mode are shown in Fig. 10. The responses for the other five modes were of smaller amplitude in comparison to the first mode. For all the three instantaneous angles of attack, the wing reached a steady aeroelastic equilibrium position within approximately 3.5 s.

For the next case, the response analysis was conducted for the transonic flow at $M = 0.72$ and $\alpha = 3.7$ deg and an altitude of 33,000 ft. At these conditions, some oscillations were observed in the flight test of the B-1 aircraft.[1,2] Response computations were initiated by giving an arbitrary unit displacement to the first generalized coordinate $q(1)$. Then aerodynamic and structural equations of motion were simultaneously integrated in time until a steady aeroelastic equilibrium state was reached. This required about 10,000 time steps of size 0.02, which corresponds to 6 s of physical time at the altitude of 33,000 ft. The response time was

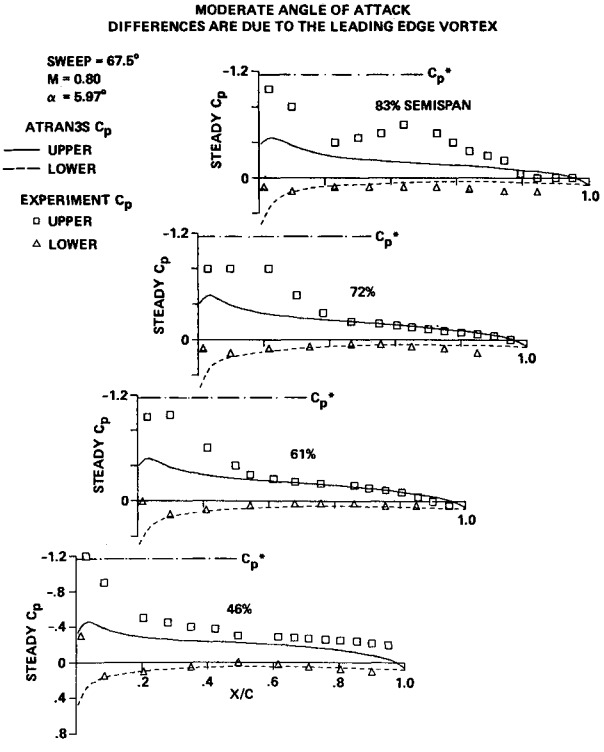

Fig. 8 Steady pressure distributions for the 67.5 deg sweep case at $M = 0.80$ and $\alpha = 5.97$ deg.

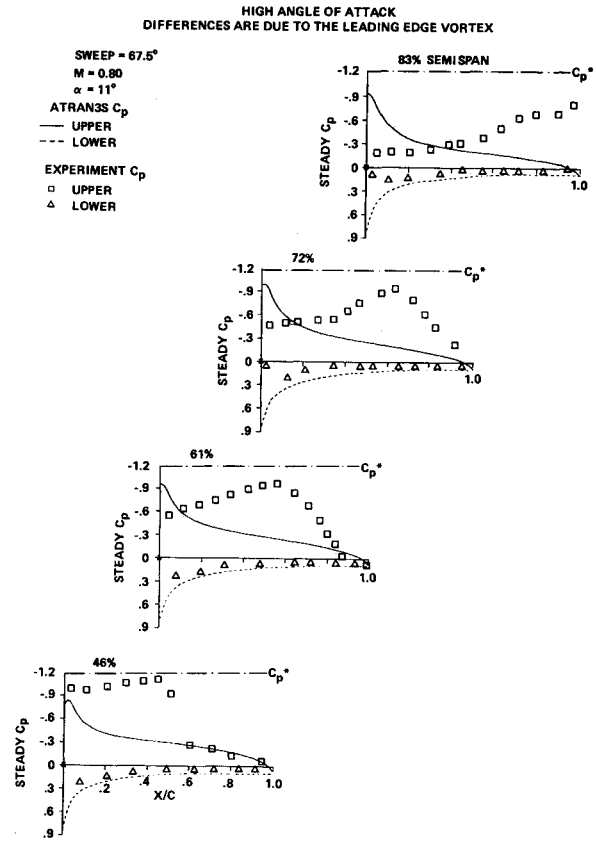

Fig. 9 Steady pressure distributions for the 67.5 deg sweep case at $M = 0.80$ and $\alpha = 11.0$ deg.

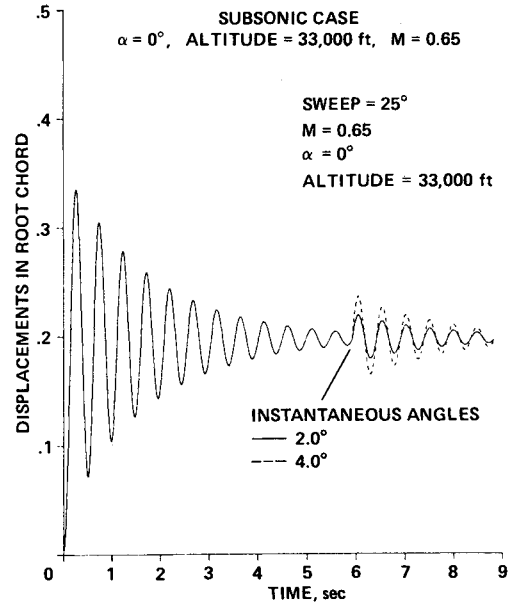

Fig. 10 Dynamic aeroelastic response of the first normal mode for the 25 deg sweep case at $M = 0.65$.

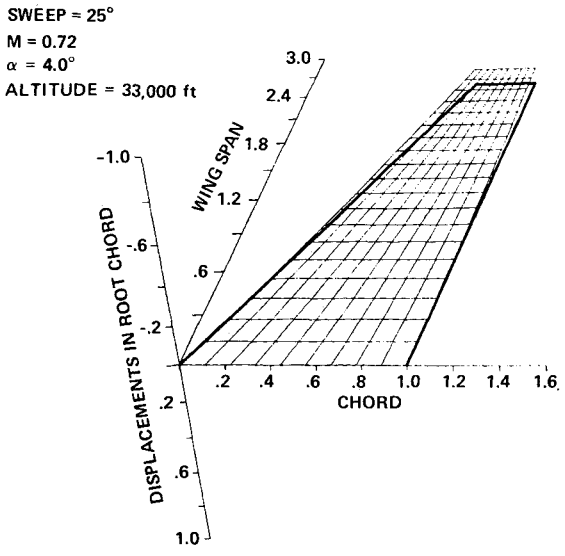

Fig. 11 Deformed shape at the static aeroelastic equilibrium position.

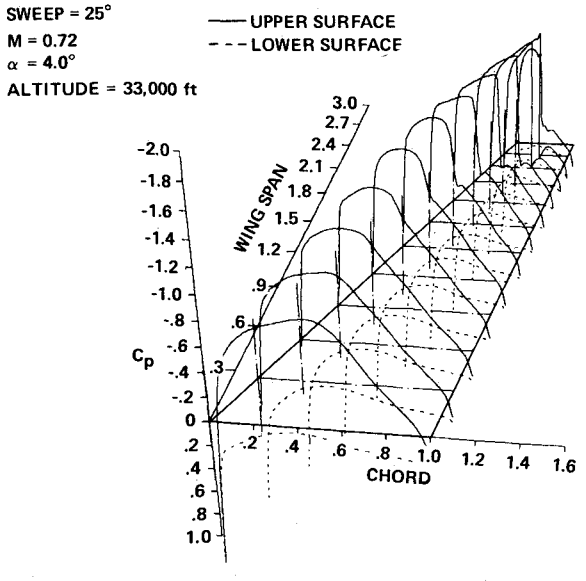

Fig. 12 Pressure distributions at the static aeroelastic equilibrium position.

similar to the subsonic case. The deformed shape of the wing at its steady aeroelastic equilibrium position is shown in Fig. 11. This deformed shape of the wing is close to the first bending mode shape of the wing. The corresponding upper- and lower-surface pressure distributions are shown in Fig. 12. A shock wave is evident on the outboard position of the upper surface of the wing.

To simulate an external disturbance to initiate oscillations, an instantaneous change in the mean angle of attack was given to the wing and the response computations were further continued. After some initial oscillations, the wing again approached a steady aeroelastic equilibrium position within 3.0 s. This required approximately 5000 time steps. Such responses were conducted for two instantaneous changes in angle of attack of 2.0 and 4.0 deg. These responses are shown for the first normal mode in Fig. 13. For both cases, the wing reaches a steady aeroelastic equilibrium position within approximately 3.0 s.

In spite of the presence of shock waves on the wing, the nature of response is similar to that observed for the subsonic case at $M=0.65$. It is noted that the wing does not pick

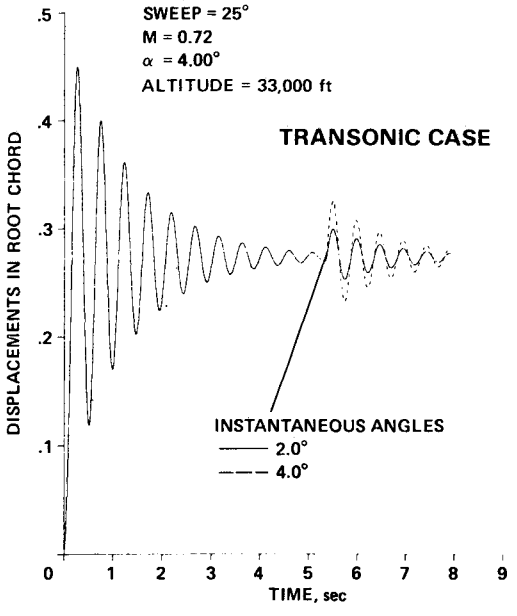

Fig. 13 Dynamic aeroelastic response of the first normal mode for the 25 deg sweep case at $M=0.72$.

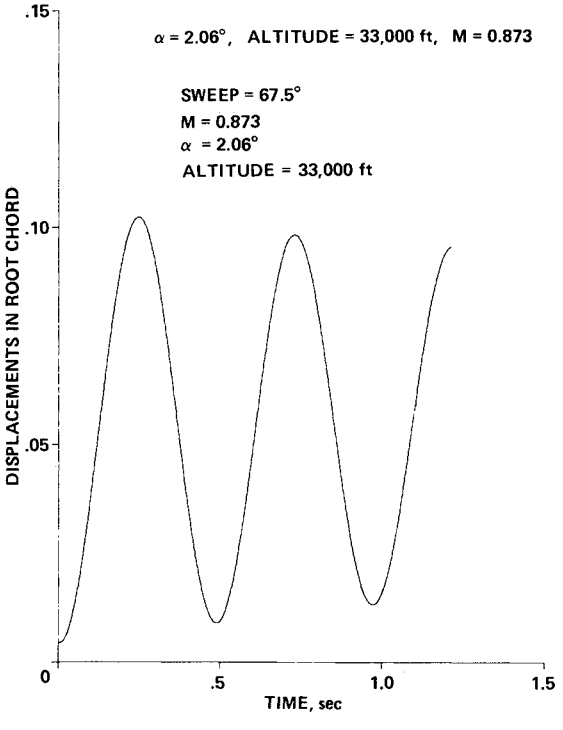

Fig. 14 Dynamic aeroelastic response of the first normal mode for the 67.5 deg sweep case at $M=0.873$.

up oscillations due to the external disturbance even when shock waves are present on the wing. However, these calculations did not simulate the effects of the shock wave interaction with the boundary layer. Hence, they could not simulate buffet, which was the cause of the oscillations observed in wind tunnel and flight tests[1,2] at these flow conditions.

For the final computation, a case at $M=0.873$ and $\alpha=2.06$ deg was selected for response analysis at the altitude of 33,000 ft. For this case, steady pressures from ATRAN3S compared favorably with the experiment as shown in Fig. 7.

Because of the low aspect ratio of 1.8 of the wing at the 67.5 deg sweep case, the time step size required was 0.002, which is 10 times smaller than the time step size required for

the 25.0 deg sweep case. Because of the large computational time required for the aeroelastic analysis, only a limited response analysis was conducted. The aeroelastic response of the first normal mode is shown in Fig. 14 for about two cycles of oscillation starting from the freestream conditions with an initial unit value for the first generalized displacement $q(1)$. The response computations that correspond to 1.35 s of physical time required about 15,000 time steps of computation. The response is damping with a very small rate. The rate of damping for this case is much smaller than those observed for the case 25.0 deg sweep. Such a low aeroelastic damping may lead to the possibility of sustained aeroelastic oscillations, as observed in the experiment.[2] Early work such as Ref. 14 (also see Chap. 9 of Ref. 13 for details) have also illustrated flutter of highly swept wings under some specific conditions. Also see the Appendix for more discussions about the reasons for oscillations.

Conclusions

The transonic code ATRAN3S was used to study the aerodynamic flow and aeroelastic response of the B-1 wing at low- and high-sweep angles of 25.0 and 67.5 deg, respectively. Steady pressures from the code compared well with experimental results in the low-sweep case for both subsonic and transonic flows. At high sweep, the comparisons were good at low angles of attack. But at higher angles of attack, the calculations did not show shock waves as had been previously proposed. An alternative source for the oscillations observed at the higher angles of attack has been proposed to be leading-edge separation vortices. A Navier-Stokes code is required to properly simulate such flows. Aeroelastic response studies showed that the damping of the wing response significantly decreased when the sweep angle was increased. The calculations using ATRAN3S were performed on a Cray X-MP computer and they required 0.46 s of CPU time to calculate one time step for a total of 1.9 h of CPU time for one complete aeroelastic response analysis for a low-sweep case.

Appendix

It had been proposed in Ref. 1 that the oscillations were due to the motion of shock waves. Wind tunnel data in Ref. 2 and our computations indicated that shock waves were absent during oscillations. Upon examination of the wind tunnel data,[2] which included pressure coefficient plots, oil flow charts, and lift curve slopes, H. Yoshihara of Boeing Military Airplane Company suggested that the oscillations were due to "the presence of leading edge separation vortices modified by secondary separation effects." Furthermore, the oscillations could be explained by the following mechanisms: "Here wing bending (primary mode) leads to outboard washout changes that cause vortex-flow loading changes (180 deg out of phase) that reinforce the bending oscillations."

A further interpretation of the oscillatory phenomenon was also given by W. J. Mykytow (retired, AFFDL) and A. M. Cunningham (General Dynamics, Fort Worth), who examined our results and data in Ref. 2. The oscillations were caused when there was an unstable transition from a two-vortex structure to a one-vortex structure as the angle of attack was increased. At the angle of attack of 7.44 deg, at which the oscillations occurred in the wind tunnel tests, the data indicated that the transition occurred with a large resulting phase lag between the wing displacement and the oscillating pressure distributions. The almost 180 deg phase lag permits work to be put into the primary bending mode and thereby into the system to sustain the oscillations. While the resulting work from this transition instability is approximately fixed, the increased wing bending response provides the counteracting stabilizing force that results in a hysteresis in the motion of the wing. A possible remedy for these oscillations would be to oscillate an aileron near the wing tip to counteract the unsteady loads due to the motion of the vortex.

Acknowledgment

We would like to thank Dr. H. Yoshihara for helpful suggestions during this work.

References

[1]Stevenson, J. R., "Shock Induced Wing Oscillation Wind Tunnel Test Results," Paper presented at Aerospace Flutter and Dynamics Meeting Conference, Williamsburg, VA, April 1984.

[2]Dobbs, S. K. and Miller, G. D., "Self Induced Oscillation Wind Tunnel Test of a Variable Sweep Wing," AIAA Paper 85-0739, April 1985.

[3]Goorjian, P. M., "Computations of Unsteady Transonic Flows," *Recent Advances in Numerical Methods in Fluids, Advances in Computational Transonics,* Vol. IV, edited by W. G. Habashi, Pineridge Press, Swansea, U.K., 1984.

[4]Ballhaus, W. F. and Goorjian, P. M., "Implicit Finite Difference Computations of Unsteady Transonic Flows about Airfoils," *AIAA Journal,* Vol. 15, Dec. 1977, pp. 1728-1735.

[5]Guruswamy, P. and Yang, T. Y., "Aeroelastic Time Response Analysis of Thin Airfoils by Transonic Code LTRAN2," *International Journal of Computers and Fluids,* Vol. 9, No. 4, Dec. 1980, pp. 409-425.

[6]Borland, C. J. and Rizzetta, D. P., "Transonic Unsteady Aerodynamics for Aeroelastic Applications, Vol. I—Technical Development Summary for XTRAN3S," AFWAL-TR-80-3107, June 1982.

[7]Guruswamy, P. and Goorjian, P. M., "Computations and Aeroelastic Applications of Unsteady Transonic Aerodynamics about Wings," *Journal of Aircraft,* Vol. 21, Jan. 1984, pp. 37-43.

[8]Seidel, D. A., Bennett, R. M., and Ricketts, R. H., "Some Recent Applications of XTRAN3S," NASA TM 85641, May 1983.

[9]Myers, M. R., Guruswamy, P., and Goorjian, P. M., "Flutter Analysis of a Transport Wing Using XTRAN3S," AIAA Paper 83-0922, May 1983.

[10]Guruswamy, P. and Goorjian, P. M., "An Efficient Coordinate Transformation Technique for Unsteady Transonic Aerodynamic Analysis of Low Aspect Ratio Wings," AIAA Paper 84-0872, May 1984.

[11]Rizzetta, D. P. and Borland, C. J., "Numerical Solution of Three-Dimensional Unsteady Transonic Flow over Wings, Including Inviscid/Viscous Interaction," AIAA Paper 82-0352, Jan. 1982.

[12]Guruswamy, P., Marstiller, J. W., Yang, T. Y., and Goorjian, P. M., "Effects of Viscosity and Modes on Transonic Flutter Boundaries of Wings," *Journal of Aircraft,* Vol. 22, Sept. 1985, pp. 756-762.

[13]Bisplinghoff, R. L., Ashley, H., and Halfman, R. L., *Aeroelasticity,* Addison-Wesley, Reading, MA, Nov. 1957.

[14]Cunningham, H. J., "Analysis of Pure Bending Flutter of a Cantilever Swept Wing and Its Relation to Bending-Torsion Flutter," NACA TN 2461, 1951.